

Comment on "Determination of Nucleus Density in Semicrystalline Polymers from Nonisothermal Crystallization Curves"

José A. Martins*

Departamento de Engenharia de Polímeros, Universidade Do Minho, Campus de Azurém, 4800 058 Guimarães, Portugal

Macromolecules 2015, 48, 2561–2569. DOI: 10.1021/acs.macromol.5b00275

S Supporting Information

Besides orientation effects induced by flow, mechanical and optical properties of semicrystalline polymers are strongly affected by the spherulite size, hence the nucleation density. Therefore, tools to predict nucleation density and to relate it to the final mean spherulite size in processed plastic parts are technologically important. Menyhárd et al.¹ presented a method for determining the nucleation density in non-isothermal crystallization experiments in the absence of flow using two sets of experimental data: the spherulite growth rate measured in polarized optical microscopy experiments (POM) at different temperatures and the bare nonisothermal DSC thermogram at a prespecified cooling rate. Before discussing this work, it must be mentioned that a procedure for dealing with this issue was published by the present author in 2002 for isothermal DSC experiments² and in 2003 for nonisothermal experiments, including the application to real processing conditions in the absence of flow.³ Errors resulting from calibration effects, the sample thermal resistance, and heat released during isothermal, nonisothermal, and shear-induced crystallizations were also considered.^{4,5}

The starting equation of ref 1 is the free-growth overall volume fraction transformed to the solid (crystalline) phase

$$X'(t) = kt^3 = \bar{N} \frac{4\pi}{3} (Gt)^3 \quad (1)$$

where k is the kinetic constant, \bar{N} the mean number of activated nuclei per unit volume of untransformed material, G the spherulite growth rate, and t the crystallization time. An instantaneous nucleation of spheres was assumed. In ref 1 $X'(t)$ was defined as "the expected volume of crystalline phase", while it is a fraction of volume (or mass) transformed to the solid phase.

The impingement effect between the solid growth fronts is evaluated in the framework of the Komolgoroff–Avrami–Evans equation^{6,7}

$$X(t) = 1 - e^{-kt^n} \quad (2)$$

A nonlinear fit of eq 2 to the experimental data yields the k and n parameters. Often, the half-crystallization time $t_{50\%}$ is defined at $X = 0.5$, and the k constant, at this specific time, is

$$k = \ln 2 / t_{50\%}^n \quad (3)$$

In ref 1, apparently inspired by another work,⁸ assuming an instantaneous nucleation of spheres, the following relation is established:

$$kt^3 = \frac{\ln(2)t^3}{t_{50\%}^3} = \bar{N} \frac{4\pi}{3} G^3 t^3 \quad (4)$$

Although mathematically correct, the equation is physically questionable. The problem relies in the product of the different equations by t^3 which assigns to kt^3 the physical meaning of a free-growth volume fraction converted to the solid phase. In fact, as shown previously,^{2,3} and summarized in the Supporting Information, a relationship between a global crystallization parameter ($t_{50\%}^{-1}$) and a local crystallization parameter (G) may be established, without the need of the above physically questionable procedure, providing that a temperature dependence for the nucleation density is assumed, and inserted, together with the temperature dependence of G , in eq S1 of the Supporting Information: $t_{50\%}^{-1} \propto \bar{N}(T)^{1/3}G(T)$.

Contrary to this procedure, in ref 1 the nucleation density is evaluated from $k = 4\pi\bar{N}G^3/3$, yielding eq 5 in ref 1: $\bar{N} = 3k/4\pi G^3$. Note that this \bar{N} evaluation relies upon the definition of the kinetic constant k , being implicit a constant crystallization temperature and an instantaneous nucleation of spheres, implying therefore that \bar{N} is immutable: it represents the number of nuclei per unit volume of untransformed material activated at the start of the process for a specific crystallization temperature.

In ref 1, \bar{N} is represented by N , and it is wrongly considered as the number of nuclei, while it is in fact a number density of nuclei. Any doubts remaining on this issue may be clarified by reading the original works, ref 6, page 212, ref 7, page 372, or still in refs 9–11.

Probably as a result of this confusion, eq 13 is written $\Delta V_{cr} = 4\pi\bar{N}(G_{Ti})^3/3$ —here expressed as a function of \bar{N} , which is physically wrong since it is dimensionally incorrect. In summary, the physically questionable relationship established in eq 4 is amplified by the physically wrong eq 13, which propagated to eqs 14 and 17 and finally, at the fourth page of ref 1, to eq 18 that the authors recognize impossible to be used for evaluating the nucleation density "because it describes the crystallization as the development of freely growing spheres". The authors cope with this problem through an unexplained correction, eq 19, that is lumped to eq 14, yielding the final equation, eq 20, which is used to evaluate the nucleation

Received: July 21, 2015

Revised: August 2, 2015

Accepted: September 29, 2015

Published: October 2, 2015



density! It turns out that N_t in eq 20 of ref 1 is dimensionally a number, not a number density.

As an outcome of these biased procedures, unacceptable predictions for the nucleation density are made. To demonstrate this statement, we consider Figures 2 and 6 of ref 1. Both refer to the same polymer. Spherulitic structures in Figure 2 refer to an isothermal crystallization at 132 °C. The half-crystallization temperature for the nonisothermal crystallization at −10 °C/min in Figure 6 is $\approx 386 \text{ K} = 113 \text{ °C}$. Clearly, the mean spherulite size for the nonisothermal crystallization experiment must be lower than the mean spherulite size after a crystallization at 132 °C.

According to Figure 6 of ref 1, and assuming that the nucleation density stabilizes at $9 \times 10^8 \text{ nuclei/m}^3$, one concludes that the volume of a single nucleus is $1.11 \times 10^{-9} \text{ m}^3$. From this value, a crude estimation of the mean spherulite diameter is 1285 μm , larger than the whole size of Figure 2, width \times height = 1142 $\mu\text{m} \times 776 \mu\text{m}$ (values evaluated from the scale provided in the figure).

An accurate comparison between data in the two figures requires the conversion of the volume density to a surface density of nuclei. This can be accomplished by using the Voronoi tessellations generated by Poissonian point distributions. Analytical expressions for first-order moments of a 3-D Poisson–Voronoi tessellation with nucleus density of \bar{N}_t were obtained by Milles¹² [*The Random Division of Space*] and Möller¹³ [*Lectures On Random Voronoi Tessellations*], in good agreement with computer experiments.^{14,15} The stereological properties of the tessellation, namely the characteristics of plane sections through 3-D tessellations, may be inferred from the statistical distributions of Poisson–Voronoi cells. According to the literature, the resulting equations were obtained by J. L. Meijering in 1953, in a work entitled “Interface area, edge length and number of vertices in crystal aggregates with random nucleation” [*Phillips Res. Rep.* **1953**, *8*, 270–290]. This work is inaccessible, but the results obtained may be found in the section 5 of ref 12 and in Table 4.2.2, page 100, of ref 13. A summary of the moments of 2-D sections through 3-D Poisson–Voronoi tessellations is presented in Table 2 of ref 14. For the present situation, the desired relationship, between the surface density and volume density of cells, is

$$\bar{\sigma} = \frac{\Gamma(1/3)(16\pi^5 \bar{N}_t^2/9)^{1/3}}{15} = 1.458 \bar{N}_t^{2/3} \quad (5)$$

where Γ is the Gamma function and $\bar{\sigma}$ the surface density of nuclei.

The equivalent surface density for the data in Figure 6 of ref 1 is $\bar{\sigma} = 1.458(9 \times 10^8)^{2/3} = 1.359 \times 10^6 \text{ nuclei/m}^2$. Each nucleus occupies an area of $7.358 \times 10^{-7} \text{ m}^2$, and its average diameter that may be directly compared with Figure 2 is $\approx 968 \mu\text{m}$. Clearly the predicted density of nuclei in ref 1 is largely underestimated. Assessment for the correct order of magnitude of this nucleation density may be directly obtained from data in Figure 2 of ref 1.

For this purpose, the Gundersen’s tilling rule, or “unbiased counting frame”, is used. For a description of this procedure see page 72 of ref 16. As shown in Figure S4 of the [Supporting Information](#), the figure is dissected, and acceptance and forbidden lines are drawn (green and black lines, respectively, in Figure S4). Spherulites crossed by the forbidden lines are rejected. From the counting in each one of the four sections a mean number of 11.75 spherulites is evaluated in an area of

$(1142 \times 776)/4 \mu\text{m}^2$, thus yielding a surface density of $5.3 \times 10^7 \text{ nuclei/m}^2$. The corresponding volume density of nuclei evaluated from eq 5 is $\bar{N}_t = 2.19 \times 10^{11} \text{ nuclei/m}^3$ for the crystallization temperature of 132 °C, in agreement with results obtained, also for iPP, by the present author³ (see Figure S1 of the [Supporting Information](#)) and by others¹⁷ (for further discussion see [Supporting Information](#)). It implies that the nucleation density for samples of the same polymer crystallized after a cooling of −10 °C/min should be around 10^{12} – $10^{13} \text{ nuclei/m}^3$ —at least 4 orders of magnitude higher than the value evaluated in Figure 6 of ref 1.

■ ASSOCIATED CONTENT

Supporting Information

The Supporting Information is available free of charge on the [ACS Publications website](#) at DOI: [10.1021/acs.macromol.5b01618](https://doi.org/10.1021/acs.macromol.5b01618).

Summary of the procedure used to evaluate the nucleation density in polymers crystallizing in the absence of flow from optical microscopy and DSC data is presented, supported by result shown in Figures S1–S3; Figure S4: an analysis of Figure 2 of ref 1 used to illustrate the nucleation density evaluation ([PDF](#))

■ AUTHOR INFORMATION

Corresponding Author

*E-mail: jamartins@dep.uminho.pt.

Notes

The authors declare no competing financial interest.

■ REFERENCES

- (1) Menyhárd, A.; Bredács, M.; Simon, G.; Horváth, Z. *Macromolecules* **2015**, *48*, 2561–2569.
- (2) Martins, J. A.; Cruz Pinto, J. J. C. *Polymer* **2002**, *43*, 3999–4010.
- (3) Martins, J. A.; Cramez, M. C.; Oliveira, M. J.; Crawford, R. J. *Macromol. Sci., Part B: Phys.* **2003**, *42*, 367–385.
- (4) Martins, J. A.; Malheiro, M. J. A.; Teixeira, J. C.; Cruz Pinto, J. J. C. *Thermochim. Acta* **2002**, *391*, 97–106.
- (5) Martins, J. A.; Zhang, W.; Carvalho, V.; Brito, A. M.; Soares, F. O. *Polymer* **2003**, *44*, 8071–8079.
- (6) Avrami, M. J. *Chem. Phys.* **1940**, *8*, 212–224.
- (7) Evans, U. R. *Trans. Faraday Soc.* **1945**, *41*, 374–380.
- (8) Lamberti, G. *Polym. Bull.* **2004**, *52*, 443–449.
- (9) Schultz, J. M. *Polymer Crystallization: The Development of Crystalline Order in Thermoplastic Polymers*; American Chemical Society: Washington, DC, 2001.
- (10) Wunderlich, B. *Macromolecular Physics*; Academic Press, New York, 1976; Vol. 2.
- (11) Janeschitz-Kriegl, H. *Crystallization Modalities in Polymer Melt Processing*. Springer: New York, 2010.
- (12) Milles, R. E. *Suppl. Adv. Appl. Prob.* **1972**, *4*, 243–266.
- (13) Möller, J. *Lectures on Random Voronoi Tessellations*; Springer-Verlag: Berlin, 1994.
- (14) van de Weygaert, R. *Astron. Astrophys.* **1994**, *283*, 361–406.
- (15) Tanemura, M. *Forma* **2003**, *18*, 221–247.
- (16) Howard, C. V.; Reed, M. *Unbiased Stereology: Three-Dimensional Measurement in Microscopy*, 2nd ed.; BIOS Scientific Publishers: Milton Park, UK, 2005.
- (17) Janeschitz-Kriegl, H. *Colloid Polym. Sci.* **2003**, *281*, 1157–1171.

Supporting Information

for

Comment on “Determination of Nucleus Density in Semicrystalline Polymers from Nonisothermal Crystallization Curves”

José A. Martins

Departamento de Engenharia de Polímeros

Campus de Azurém

4800 058 Guimarães

Portugal

jamartins@dep.uminho.pt

Contents:

Supporting Text

Figures S1, S1, S3, S4

Supporting References

Supporting Text

This text presents a summary of the procedure described with detail in previous works to evaluate the nucleation density in polymers crystallizing in the absence of flow. This evaluation was done by relating local and global crystallization experimental results. The former, performed in a hot-stage coupled to an optical microscope, provides information on the spherulite growth rate. The latter allows recording the overall crystallization kinetics.

Regardless the nucleation type, instantaneous or sporadic, as demonstrated in Fig. S1, there is always significant impingement between spherulites, long before the attainment of the half-crystallization time. In the framework of Avrami's equation for an instantaneous nucleation of spheres, accounting for the effect of impingement between spherulites in the solidification process implies the following relation between $t_{50\%}$ and k

$$t_{50\%}^{-1} = \left(\frac{k}{\ln 2} \right)^{1/3} = \left(\frac{4\pi\rho_s}{3\rho_l} \frac{\bar{N}}{\ln 2} \right)^{1/3} G. \quad (\text{S1})$$

At high temperatures, nucleation (either primary or secondary) is the slowest process, and this temperature dependence is generally expressed by

$$t_{50\%}^{-1} \propto G \propto \exp\left(-\frac{K_g}{T\Delta T f}\right). \quad (\text{S2})$$

To explain the different slopes - K_g - values, as well as the vertical shift, when $\ln(t_{50\%}^{-1})$ and $\ln(G)$ are both plotted as function of $(T\Delta T f)^{-1}$, as shown in Fig. S2a, a dependence of the nucleation density on the temperature has to be considered. It was neglected in a latter work⁸ that obtained a similar relationship for estimating the nucleation density by coupling global and local crystallization experimental results. Problems with the reasoning there used were mentioned in the main paper. Establishment of this dependency is crucial for assigning a physical meaning to the obtained final result.

Crystallization models, such as Avrami's equation, do not explicitly consider this dependence. It is aggregated, together with the temperature dependence of G , in the k parameter.

It was assumed that the temperature dependence of \bar{N} is proportional to the probability of formation of a nuclei with critical size, that this nuclei develops in a heterogeneous substrate, and that this development is coherent with the substrate.² The proportionality factor, although

important from both an experimental and theoretical point of view, because it determines the maximum attainable nucleation density, is not relevant here since, as shown below, it is included in the pre-exponential factor of $(t_{50\%}^{-1})_0$. A more detailed accounting for this dependence was given in ref. S1, where an equilibrium distribution of nuclei is evaluated.

Assuming then that

$$\bar{N} \propto \exp\left(-\frac{K_n}{T\Delta T f}\right), \quad (\text{S3})$$

eq. (S1) may be written as

$$\ln t_{50\%}^{-1} = \ln(t_{50\%}^{-1})_0 - \frac{\Delta G_d}{RT} - \left(\frac{K_n}{3T\Delta T f} + \frac{K_g}{T\Delta T f}\right), \quad (\text{S4})$$

or, since $K_n = K_g \equiv K_g^G$ (because of the same nucleation type and coherence with the substrate),

$$\ln t_{50\%}^{-1} = \ln(t_{50\%}^{-1})_0 - \frac{\Delta G_d}{RT} - \left(\frac{K_g^{1/t_{50\%}}}{T\Delta T f}\right), \quad (\text{S5})$$

with

$$\ln(t_{50\%}^{-1})_0 = \frac{1}{3} \ln\left(\frac{4\pi\rho_s}{3\rho_l} \frac{N_0}{\ln 2}\right) + \ln G_0,$$

and

$$K_g^{1/t_{50\%}} = \frac{4}{3} K_g^G, \quad (\text{S6})$$

where K_g^G is the slope of $\ln(G)$ as function of $(T\Delta T f)^{-1}$.

Equation (S6) can be used as a gauge to infer the nucleation type and the dimensionality of the growing structure from experimental DSC and optical microscopy data. This inferring is free from model assumptions, other than that both nucleation and growth are interface controlled processes involving the same interface energies. For an instantaneous nucleation of structures having the spherical shape, the ratio between the two, expressed by eq. (S6) is 1.333. For POM and iPP in Fig. S2a, that ratio is 1.12 and 1.253, respectively^{2,3}, while for other polymers, such as MPDE, it is 1.283.²

The vertical shift between $\ln(t_{50\%}^{-1})$ and $\ln(G)$ yields the semi-empirical nucleation density variation with

$$\bar{N}_t = \frac{3 \ln(2)}{4\pi} \left\{ \left(\frac{(t_{50\%}^{-1})_0}{G_0} \right)^3 + \exp \left[\frac{3(K_g^G - K_g^{1/t_{50\%}})}{T \Delta T f} \right] \right\}, \quad (S7)$$

which is eq. (13) of ref. 2. Figure S2b shows predictions confirmed by experimental data. Differences between them are more perceptible at lower crystallization temperatures and may be assigned to the DSC instrument's lack of sensitivity for detecting the heat released at the very earlier crystallization stages.

Extension of this procedure to nonisothermal experiments was also performed.³ The nonisothermal crystallization data was corrected for the calibration on cooling and for the heat released during the crystallization (both isothermal and nonisothermal). None of these two corrections was considered by the authors in refs. 1 and 8. A temperature $T_{50\%}$, corresponding to the half of the phase change, was evaluated, and its value was located in the plots in Fig. 2a, from which a nucleation density was estimated – Fig. S3. The values obtained were then compared with others evaluated from plastic parts processed by rotational moulding, enabling a prediction of the final spherulite size illustrated in Fig. S3. Application of this procedure to injection moulding parts, would be, at best, limited to the core spherulitic structure, even though requiring knowledge of the cooling rate at different sections of the part.

Although the nucleation density might change for different iPP grades, depending on the nucleating agents used, its dependency on the supercooling degree is illustrated in Fig. 5 of ref. 16. From data in that figure it can be seen that predicted nucleation density for a quiescent crystallization at 132 °C ($\log \Delta T \approx 1.9$) is higher than 10^{10} nuclei/m³ and that corresponding to 113 °C ($\log \Delta T \approx 2.0$) is around 10^{13} nuclei/m³, far above than the estimate made in Fig. 6 of ref. 1.

Since one reviewer raised doubts on the applicability of combined DSC and optical microscopy results to predict the nucleation density in nonisothermal experiments, arguing that the above procedure is “not on sound scientific foundation” because “under temperature gradients polymers exhibit directional crystallization” and “when confined by DSC pans, the surface nucleation plays a significant role in crystallization”, the following clarifications are in order.

The only way to ascertain the validity of a predictive method, and therefore its scientific foundations, is to compare their predictions with experimental results for a variety of materials as wide as possible, and for different working conditions, in this case, isothermal and nonisothermal

crystallization experiments in the absence of flow. Squares and circles in figs. S2b and S3 are nucleation density values measured on microtomed sections of samples crystallized in a DSC under isothermal or non-isothermal conditions. The measurements were made either by SALS or by the method described in Fig. S4. SALS measurements yield a mean spherulite diameter, representative of all structures hit by the spot (including eventual surface nuclei), from which a nucleation density can be directly evaluated. As can be seen, predictions compare well with experimental results. Those predictions were also extended to 10 mm thick plastic parts processed by rotational moulding.³ The cooling rates at 1 mm, 3 mm, 5 mm, 7 mm and 9 mm from the mould wall were measured by thermocouples inserted in the plastic part. From these cooling rates, a temperature $T_{50\%}$ corresponding to half of the phase change was evaluated, and using eq. (S.7) the nucleation density was predicted.

For samples of thickness around 1 mm, and in the absence of any thermal event in the sample, the temperature difference between the sample bottom and top, exclusively due to the sample's thermal resistance, is around 2 °C for highest cooling rate used (≈ -32 °C/min).⁴ The thermal gradients existing in DSC samples cooled at -32 °C/min are then around 2 °C/mm. The combined effects of the sample thermal resistance and heat of crystallization released during the phase change may be evaluated (see Fig. 10 in ref. S2) and, for each cooling rate a $T_{50\%}$ defined and used as above to estimate the nucleation density. So far, all known estimates made following the above procedure agreed with experimental nucleation density results (within the error bars, as shown in Fig S3).

As for the scientific foundations of the method, the following has to be said. Global crystallization experiments such as those performed in a DSC measure the heat released during the phase change at a predefined temperature or cooling rate. To describe the integrated results, different physically sound models may be used. One most used is the Avrami's equation. The kinetic constant of the Avrami's equation is proportional to $\bar{N}G^3$. It turns out that Avrami's model implicitly considers \bar{N} (the nucleation density) as a temperature independent value. It is known from experiments that increasing the supercooling degree increases the nucleation density.

The modification made that allowed the implementation of the predictive method and writing eq. (S7) was to assume that the temperature dependence of \bar{N} is proportional to the probability

of formation of a nuclei with critical size, that this nuclei develops in a heterogeneous substrate, and that this development is coherent with the substrate.

Despite the good agreement of eq. (S.7) with experimental results for the nucleation density, this procedure is not of universal validity. Extension of this methodology to samples crystallized at very low supercoolings will fail due to the extensive development of transcrystalline layers as a result of the enhanced surface nucleation. Still to explore, is the application of this procedure to predict the nucleation density in samples crystallizing at very high cooling rates, or to crystallizations from the glass. For flow induced crystallization processes, this method might eventually work for predicting the mean spherulite size of the core spherulitic structures in injection moulded parts providing that mean cooling rates could be defined at different sections of the part.

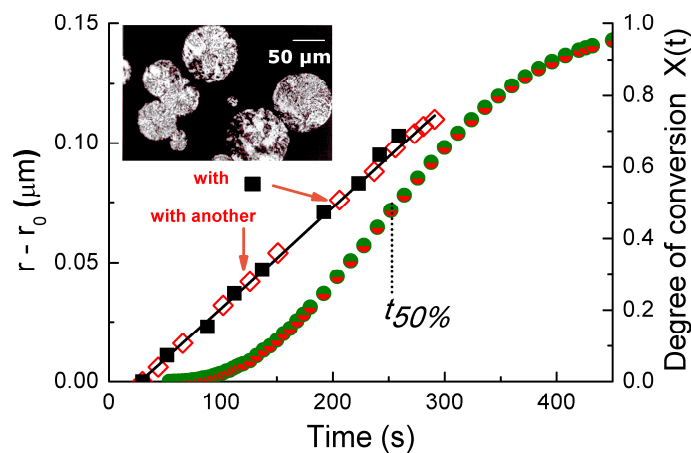


Figure S1. Isothermal crystallization of polyoxymethylene at 157 °C in a hot-stage and in a DSC. Time zero was set at the start of the isothermal in both instruments. The picture at the inset was taken in a polarized optical microscope during the crystallization at 157 °C and it corresponds to a crystallization time of 235 s. Diamonds and squares refer to measurements on the two spherulites at the lower right. The transformed area in the figure is around 45%. The impingement between spherulites is evident long before the half of crystallization time as it is evident the sporadic nature of the nucleation in POM at 157 °C.

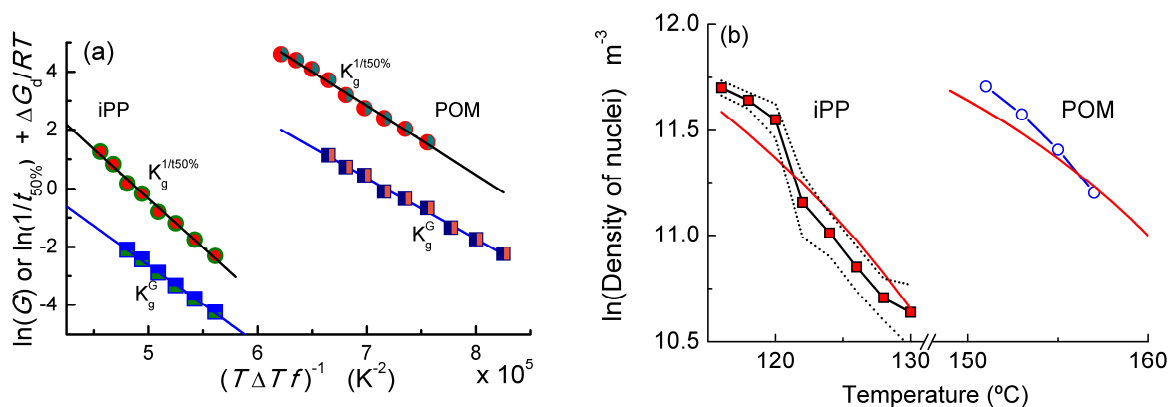


Figure S2. Use of combined DSC and optical microscopy data to evaluate the nucleation density. (a) Representation of the spherulite growth rate data and reciprocal of half crystallization time at different crystallization temperatures for POM² and iPP.³ The vertical shift between $\ln(t_{50\%}^{-1})$ and $\ln(G)$ yields the nucleation density represented in (b). Dotted lines in (b) indicate the errors in the experimental nucleation density evaluation of iPP (squares) and POM (circles), which was made by analysing microtomed sections of crystallized DSC samples.

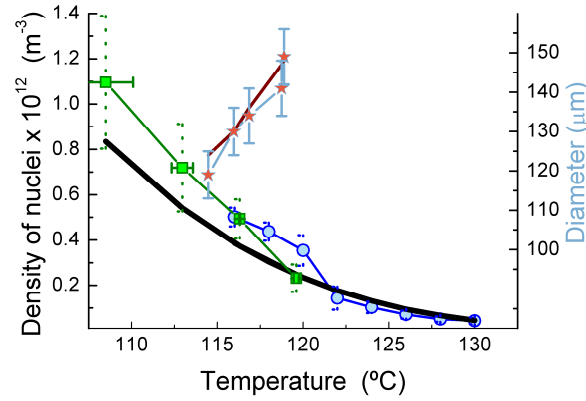


Figure S3. Prediction of nucleation density for isothermal and nonisothermal experiments and its use for evaluating the final mean spherulite diameter in real processing conditions. Black thick line is the prediction in a wide temperature range encompassing both isothermal and nonisothermal experiments. Squares are experimental evaluations for the nucleation density made for nonisothermal experiments at cooling rates from -5 °C/min up to -32 °C/min. Samples were crystallized in a DSC at the above cooling rates, and the microtomed sections analysed either by SALS or by the method described in Fig. S4. The corresponding temperatures were evaluated at half of the solidification process ($T_{50\%}$). The vertical error bars results represent errors in the evaluation of the nucleation density while the horizontal error bars stand for the combination of calibration on cooling errors and the sample thermal resistance effect on the $T_{50\%}$ definition. Circles are the experimental nucleation density values for isothermal experiments already presented in Fig. 2b. Measurements of the final spherulite size in parts processed by rotational moulding are shown by stars while the line is the corresponding prediction.³

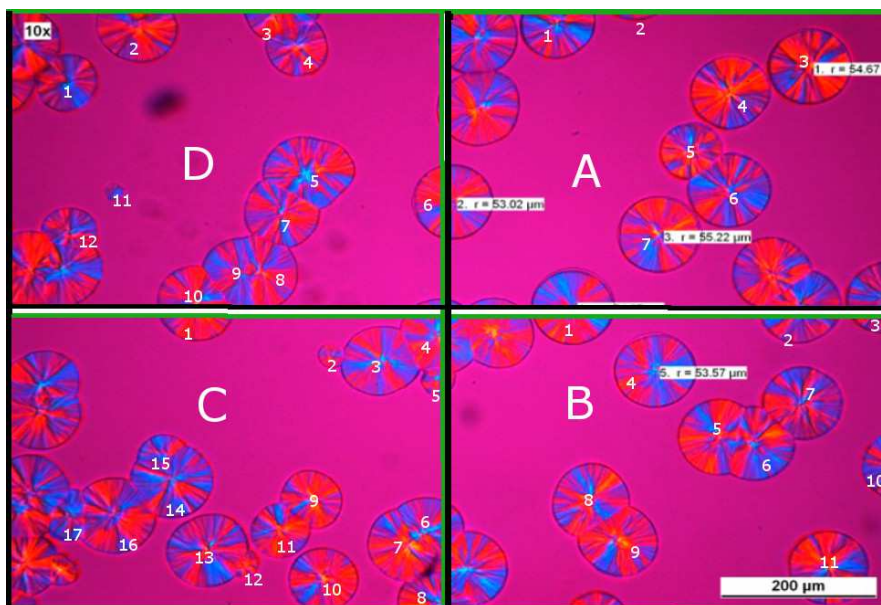


Figure S4. Figure 2 of ref. 1 for the isothermal crystallization at 132 °C. To evaluate the nucleation density, the figure was divided in four equal sections A to D. For each section acceptance lines (green) and forbidden lines (black) are drawn. Spherulites crossed by the forbidden lines are not counted. The number of spherulites in each section are: A – 7, B – 11, C – 17 and D – 12, the mean number being 11.75 per section. The overall figure area, evaluated from the scale drawn the authors is $1142 \times 776 \mu\text{m}^2$. The surface density of nuclei is 5.3×10^7 nuclei/ m^2 corresponding to a volume density of $\bar{N}_t = 2.19 \times 10^{11}$ nuclei/ m^3 .

References

- (S1) Muthukumar, M. *Nucleation in polymer crystallization*. Advances in Chemical Physics, **2004**, 128, 1-63.
- (S2) Malheiro, M. J. A., Martins, J. A., Cruz Pinto, J. J. C. *Thermochim. Acta* **2004**, 420, 155-161.